Ultrafast THz photophysics of solvent engineered triple-cation halide perovskites

Kumar, Abhishek; Priyadarshi, Anish; Shukla, Sudhanshu; Manjappa, Manukumara; Haur, Lew Jia; Mhaisalkar, Subodh Gautam; Singh, Ranjan

2018

Kumar, A., Priyadarshi, A., Shukla, S., Manjappa, M., Haur, L. J., Mhaisalkar, S. G., & Singh, R. (2018). Ultrafast THz photophysics of solvent engineered triple-cation halide perovskites. Journal of Applied Physics, 124(21), 215106-. doi:10.1063/1.5051561

https://hdl.handle.net/10356/82964

https://doi.org/10.1063/1.5051561

JOURNAL OF APPLIED PHYSICS **124**, 215106 (2018)

Ultrafast THz photophysics of solvent engineered triple-cation halide perovskites

Abhishek Kumar,[1] Anish Priyadarshi,[2,3,a)] Sudhanshu Shukla,[3,4] Manukumara Manjappa,[1] Lew Jia Haur,[3] Subodh G. Mhaisalkar,[3,4] and Ranjan Singh[1,a)]
[1]*Division of Physics and Applied Physics, School of Physical and Mathematical Sciences, Nanyang Technological University, 21 Nanyang Link, Singapore 637371, Singapore*
[2]*Department of Physics and Technology, UiT The Artic University of Norway, 9037 Tromsø, Norway*
[3]*Energy Research Institute @ NTU (ERI@N), Research Techno Plaza, X-Frontier Block, Level 5, 50 Nanyang Drive, Singapore 637553, Singapore*
[4]*School of Materials Science and Engineering, Nanyang Technological University, Nanyang Avenue, Singapore 639798*

(Received 9 August 2018; accepted 17 November 2018; published online 7 December 2018)

Solution processed thin film organic-inorganic perovskites are key to the large scale manufacturing of next generation wafer scale solar cell devices. The high efficiency of the hybrid perovskite solar cells is derived mainly from the large carrier mobility and the charge dynamics of films, which heavily depend on the type of *solvent* used for the material preparation. Here, we investigate the nature of *conduction and charge carrier dynamics* of mixed organic-inorganic cations [methylammonium (MA), formamidinium (FA), and cesium (Cs)] along with the mixed halides [iodine (I) and bromine (Br)] perovskite material [$Cs_{0.05}(MA_{0.17}FA_{0.83})_{0.95}Pb(I_{0.83}Br_{0.17})_3$] synthesized in different solvents using optical pump terahertz probe (OPTP) spectroscopy. Our findings reveal that carrier mobilities and diffusion lengths strongly depend on the type of solvent used for the preparation of the mixed cation perovskite film. The mixed cation perovskite film prepared using dimethylformamide/dimethylsulfoxide solvent shows greater mobility and diffusion length compared to γ-butyrolactone solvent. Our findings provide valuable insights to improve the charge carrier transport in mixed cation perovskites through solvent engineering. *Published by AIP Publishing.* https://doi.org/10.1063/1.5051561

I. INTRODUCTION

Hybrid organic-inorganic perovskite (HOIP) materials have gained immense interest in the field of solar energy conversion and other optoelectronic applications such as light emitting devices, lasing, photonic devices, and laser cooling.[1–6] These perovskite materials have distinct features that include high optical absorption across the visible spectrum, long electron and hole diffusion lengths in the range of micrometers, high carrier mobilities, low exciton binding energies, low defect density, and bandgap tunability by halide and cation substitution.[7–9] However, one of the several challenges to realize practical applications using the perovskite materials is their environmental stability. Perovskite compositional engineering through substitution and/or mixing of cations and halides offers a broad window of performance optimization for different photovoltaic applications. Mixing of smaller inorganic cation, such as Cs, has proven to be more effective in stabilizing the phase owing to its smaller size, which provides more space for the formation of the desirable photoactive perovskite phase α-(black). Recently, mixed organic-inorganic cations (methylammonium, formamidinium, and cesium) along with the mixed halides (iodine and bromine) perovskite material [$Cs_x(MA_{0.17}FA_{0.83})_{(1-x)}Pb(I_{0.83}Br_{0.17})_3$] have emerged as promising candidates for perovskite solar cells (PSCs) that have achieved high solar conversion efficiency (>21%) and have simultaneously addressed the problem of thermal and phase instability.[10] This opens up an exciting opportunity to investigate the fundamental charge carrier transport mechanisms under the equilibrium and the non-equilibrium conditions, where the carrier mobilities and diffusion lengths in mixed cation perovskites could be very different.

The performance of the perovskite solar cells (PSCs) is strongly dependent on the perovskite film morphology, which gives rise to different charge carrier transport mechanisms and photophysics. The use of various solvents in preparing the solution such as dimethylformamide (DMF), γ-butyrolactone (GBL), and dimethylsulfoxide (DMSO) plays an important role in achieving uniform and dense perovskite layers, which in turn affects the efficiency of perovskite solar cells.[11–13] The choice of solvent depends on the type of perovskite and the device architecture as well; for example, GBL has been commonly used in carbon based hole conductor free perovskite solar cells along with 5-ammonium valeric acid iodide (AVAI) additive, while DMF/DMSO is used in conventional perovskite solar cells to achieve high performance in the respective systems.[10,11,14]

Here, in this work, we studied the mixed cation organo-lead halide perovskite $Cs_{0.05}(MA_{0.15}FA_{0.85})_{0.95}Pb(I_{0.85}Br_{0.15})_3$ prepared using two different solvents, namely, DMF/DMSO and GBL and investigated their charge carrier dynamics by means of optical pump and terahertz probe (OPTP) spectroscopy.

a)Authors to whom correspondence should be addressed: anish.priyadarshi@uit.no and ranjans@ntu.edu.sg

Optical characterization of the perovskite thin films was performed using the nonlinear ZnTe crystal based optical pump and terahertz probe spectroscopic system, where the perovskite thin films were photoexcited using 400 nm pump beam and the dynamics of the excited charge carriers were probed by the terahertz pulse. In experiments, the diameters of both the terahertz and the optical pump beam were 4 mm and 6 mm, respectively, which ensured uniform optical excitation within the probing area. Terahertz radiation due to its low energy (1 THz = 4.1 meV) becomes the perfect candidate to probe the free carrier dynamics. In addition to this, OPTP spectroscopy technique gives both real and imaginary part of photoconductivity without the need for Kramers-Kronig transformation, which allows the extraction of the carrier density, carrier mobility, and diffusion lengths.

II. RESULTS AND DISCUSSION

A. Charge carrier mobility analysis

Perovskite thin film of mixed cations (MA/FA/Cs) along with mixed halides (I/Br) was prepared using two different solvents (DMF/DMSO and GBL) by the spin coating method. We performed the OPTP measurements of the perovskite films prepared using different solvents. In the OPTP measurement, exciting above the semiconducting energy bandgap generates free carriers that interact with terahertz (THz) probe beam, thereby reducing the transmission. Hence, monitoring the change in THz transmission ($-\Delta T/T$) allows one to investigate the photoconductivity of thin films. We excited the sample with the optical pump beam with photon energy of 3.1 eV, which is well above the bandgap of the chosen perovskite samples ($E_g \sim 1.58$ eV).[15] In order to estimate the initial mobility of the photocarriers, we calculated the peak photoconductivity using the following equation:[16]

$$\Delta\sigma(t_p) = \frac{\varepsilon_0 c}{d}(n_{air} + n_{sub})\frac{-\Delta T(t_p)}{T}, \tag{1}$$

where c is the speed of light, d is the thickness of sample, and n_{air} and n_{sub} are the refractive indices of air and substrate, respectively. At various pump fluences, the peak photoconductivity varies and increases with pump fluences. Further, using the peak conductivity values, the initial mobilities were calculated using the relation, $\mu = \Delta\sigma/q\eta N_0$, where q is the elementary charge, N_0 is the initial charge carrier densities, and η is the quantum yield of excitation, which is equal to the ratio of the induced charge-carrier density and the absorbed photon density. The initial carrier density is estimated by

$$N_0 = \frac{\alpha(\lambda)\lambda f(1 - 10^{-OD})}{hc}, \tag{2}$$

where α is the absorption coefficient at the excitation wavelength ($\lambda = 400$ nm in our case), f is the incident pump fluence, and $(1 - 10^{-OD})$ is the fraction of the pump light absorbed by the sample, where OD is the optical density given by $OD = 0.434\ \alpha l$, with l being the thickness of the sample.

Since the value of η lies between 0 and 1 ($0 \le \eta \le 1$), we extract the lower limit of charge-carrier mobility using $\eta = 1$. The extracted mobilities at various pump fluences are shown in Fig. 1, where the perovskite thin film prepared in the DMF/DMSO solution exhibits high mobility compared to the GBL solution prepared thin film. By increasing pump fluences, the mobilities decrease from 300 cm^2 $(V\,s)^{-1}$ to 80 cm^2 $(V\,s)^{-1}$ for the DMF/DMSO prepared film, while they decrease from 90 cm^2 $(V\,s)^{-1}$ to 15 cm^2 $(V\,s)^{-1}$ for the GBL prepared film. However, for both thin films, the trend of mobility as a function of pump fluence is identical to each other, which is attributed to the increase in the electron scattering rate. At higher pump fluences, the rise of free carrier density leads to Auger recombination which is mainly many body effects that increases the free carriers scattering. The relation between free carrier mobility and scattering rate is given by $\mu = e/(\Gamma m)$, where e, Γ, and m denote the elementary charge, scattering rate, and mass of free carriers, respectively. From the mathematical relation, it is clear that increasing scattering rate reduces the carrier mobility. In Fig. 1, the red solid line represents the variation of carrier mobility as a function of pump fluence for the perovskite prepared using the DMF/DMSO solvent, while the black solid curve depicts that for the GBL prepared perovskite. *The perovskite film prepared using DMF/DMSO solvent shows higher mobility compared to GBL.* It reflects the fact that the quality of thin film prepared using DMF/DMSO solvent is better than the film prepared using the GBL solvent. However, the decreasing mobility trend persists in perovskite films prepared using both solvents.

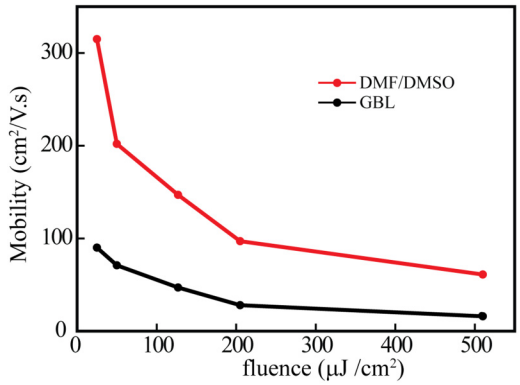

FIG. 1. Charge carrier mobilities at various pump fluences in the perovskite thin film prepared using two different solvents: DMF/DMSO and GBL.

B. Charge carrier recombination analysis

Terahertz photoconductivity is directly proportional to the product of charge carrier density and carrier mobilities. Here, we assume that the carrier mobilities do not change with pump-probe delay; hence, decay in THz transients reflects the temporal evolution of charge carrier densities after photoexcitation. In perovskites, charge carrier follows multiple decay paths, which can be mathematically described by[17–20]

$$\frac{dn}{dt} = -k_3 n^3 - k_2 n^2 - k_1 n, \tag{3}$$

where k_1, k_2, and k_3 are the monomolecular, bimolecular, and Auger recombination rate constants, respectively. "n" is the charge carrier density generated by photoexcitation in the sample which is directly proportional to the change in THz

TABLE I. Extracted recombination rate constants. The values were extracted by performing global fitting to the terahertz transients shown in Fig. 2 using Eq. (3).

Solvent	k_1 (s^{-1})	k_2 ($cm^3\ s^{-1}$)	k_3 ($cm^6\ s^{-1}$)
GBL	3×10^7–1.5×10^8	1.2×10^{-10}–6.2×10^{-10}	2.4×10^{-27}
DMF/DMSO	8.5×10^7–1×10^8	1.8×10^{-10}–2.6×10^{-10}	4×10^{-28}

transmission signal ($-\Delta T/T$). In order to extract the different decay constants, we have performed the global fitting to all THz transients using Eq. (3) as shown in Fig. 2 and the extracted values of rate constants are listed in Table I.

The terahertz transients were fitted for the range of monomolecular (k_1) and bimolecular rate constants (k_2). The identical values of monomolecular and bimolecular rate constants ensure identical diffusion length at low carrier densities (Fig. 3). At higher charge carrier concentrations, Auger recombination processes reduce the diffusion length. The perovskite film prepared using the GBL solvent exhibits higher Auger recombination rate (Table I) compared to the film prepared in the DMF/DMSO solvent. This results in a large difference in the diffusion length occuring at high carrier densities. We evaluated the diffusion length, L_D, using the extracted rate constants and initial carrier mobility. The diffusion length (L_D) is given by[19]

$$L_D = \sqrt{\frac{D}{R_{total}}},$$

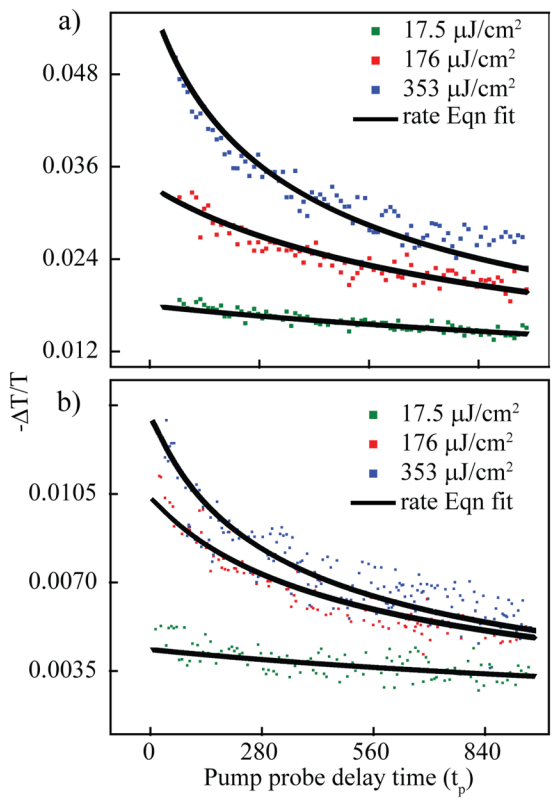

FIG. 2. THz transients at different pump fluences of perovskites prepared using (a) DMF/DMSO solvent and (b) GBL solvent. The dotted points are experimentally measured THz transients, while the black solid lines are the fits using the rate equation [Eq. (3)].

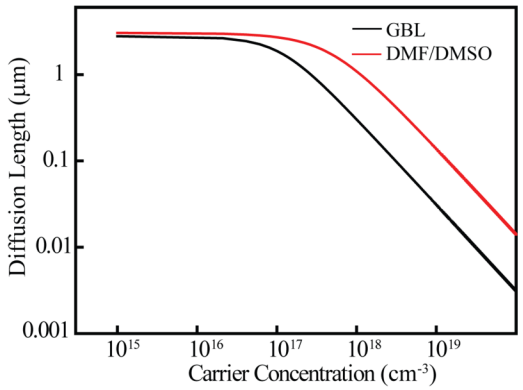

FIG. 3. Charge-carrier diffusion lengths in perovskite thin films prepared using DMF/DMSO (red solid line) and GBL solvent (black solid line), respectively, as a function of charge-carrier density.

where D is the diffusion constant given by $D=\mu k_b T e^{-1}$, here k_b, T, and e are the Boltzmann constant, temperature, and elementary charge, respectively. R_{total} is the total recombination rate which depends on the rate constants and carrier density

$$R_{total} = k_1 + nk_2 + n^2k_3.$$

Figure 3 depicts the extracted diffusion length as a function of charge carrier densities. The red and black solid lines represent the diffusion length for perovskite prepared using DMF/DMSO and GBL solvents, respectively. *It clearly exhibits the significant difference in the diffusion length at higher carrier densities which arises due to higher Auger recombination rate in the GBL solvent prepared perovskite thin film.*

The extracted mobilities and the diffusion length for the perovskite film prepared using DMF/DMSO and GBL solutions exhibit significant differences. These differences can be attributed to the difference in the film quality because of perovskite-solvent interaction. Figure 4 shows the morphology of the spin-coated perovskite films using different solvents. Clearly, the morphology appears to be strongly dependent on the choice of the solvent. The SEM images of the perovskite thin film prepared using DMF/DMSO [Fig. 4(a)] and GBL [Fig. 4(b)] solvents reveal that the film quality using the DMF/DMSO solution is much better compared to the perovskite thin film prepared using the GBL. DMF/DMSO solvent gives a compact film with bigger grain sizes, while the GBL based solvent results in a granular texture of the films. Approximate average grain size for GBL

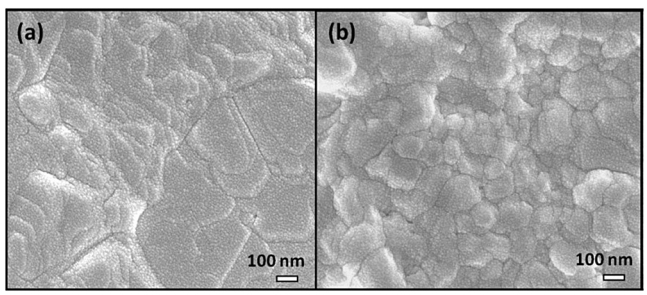

FIG. 4. SEM micrograph of the $Cs_{0.05}(MA_{0.17}FA_{0.83})_{0.95}Pb(I_{0.83}Br_{0.17})_3$ perovskite films synthesized using (a) DMF/DMSO and (b) GBL.

based triple cation perovskite film is 150–200 nm, with very few big grains of 500 nm. In the case of DMF/DMSO solvent, the average grain size is much larger (approximately 500–600 nm) with fewer grain boundaries. In general, DMF/DMSO solvent is used in the conventional (mesoporous and planar) perovskite solar cell architecture to achieve large grain size owing to its high crystallization rate and consequently resulting in a better film quality.[17,18] On the other hand, slower crystallization in the GBL solution gives more defect dominated films which, in turn, restricts the mobility and diffusion length of free carriers. However, these solutions are more useful in carbon based perovskite cells where slower crystallization rate helps in better infiltration of perovskite solution through the carbon layer in the ZrO_2 scaffold.[12,21]

The perovskite thin films using different solvents were prepared in the following way. Firstly, we prepared the mixed cation $MA_{0.17}FA_{0.87}Pb[I_{0.87}Br_{0.17}]_3$ perovskite by mixing the precursors in their respective ratio in a mixed solution of DMF/DMSO (DMF:DMSO = 4:1) and GBL in 1.35M concentration in the glove box. 0.0504 g of MABr, 0.1816 g of $PbBr_2$, 0.3872 g of FAI, and 1.1408 g. PbI_2 was first dissolved in 2 ml solution of DMF/DMSO, and GBL solution separately. Cesium containing stock solution was prepared by dissolving CsI in DMSO in 1.5M concentration. Subsequently, both solutions were mixed to get the desired solution. To obtain the desired stoichiometry, 47.6 μl of the stock CsI solution was added to 1 ml solution of the mixed cation solution and the resulting solution with a chemical formula of $Cs_{0.05}(MA_{0.17}FA_{0.83})_{0.95}Pb(I_{0.83}Br_{0.17})_3$ is obtained. Further, the perovskites layer was deposited on a quartz substrate by spin coating the precursor solvent at 1000 and 6000 rpm for 10 s and 20 s, respectively, followed by slowly dropping the 120 μl of chlorobenzene anti-solvent onto the spinning substrate in the 10th second upon reaching 6000 rpm. Finally, the sample was annealed at 100 °C on a hotplate for 30 min in a nitrogen filled glovebox.

The highest efficiencies were obtained using the DMF/DMSO solvent in the conventional device architecture.[22,23] This is in agreement with the excellent mobility and diffusion lengths obtained in our results for DMF/DMSO compared to other solvents. However, DMF solvent is classified as highly toxic and volatile which makes it inappropriate to use for high volume production of perovskite devices (either solar cell or light emitting diode).[22] These results along with the THz spectroscopy measurement method will provide guidelines to select appropriate solvents to synthesize perovskites solar cells with excellent optoelectronic properties in a safe and suitable environment.

IV. CONCLUSION

We have probed the ultrafast photophysics of solvent engineered triple cation $[Cs_{0.05}(MA_{0.17}FA_{0.83})_{0.95}Pb(I_{0.83}Br_{0.17})_3]$ perovskites prepared using DMF/DMSO and GBL solvents using OPTP measurements. Our investigation reveals that triple cation perovskites in DMF/DMSO solvent exhibit higher diffusion lengths and carrier mobilities compared to the mixed cation perovskite prepared in the GBL solvent. Such effects are likely to arise from the morphology of the perovskite film that largely depends on the choice of the solvent.

ACKNOWLEDGMENTS

The authors acknowledge the Singapore Ministry of Education (Grant Nos. MOE2017-T2-1-110 and MOE2016-T3-1-006) for funding of this research.

[1]M. A. Green, A. Ho-Baillie, and H. J. Snaith, Nat. Photon. **8**, 506 (2014).
[2]S. A. Veldhuis, P. P. Boix, N. Yantara, M. Li, T. C. Sum, N. Mathews, and S. G. Mhaisalkar, Adv. Mater. **28**, 6804 (2016).
[3]S. D. Stranks and H. J. Snaith, Nat. Nano **10**, 391 (2015).
[4]G. Xing, N. Mathews, S. Sun, S. S. Lim, Y. M. Lam, M. Grätzel, S. Mhaisalkar, and T. C. Sum, Science **342**, 344 (2013).
[5]G. Xing, N. Mathews, S. S. Lim, N. Yantara, X. Liu, D. Sabba, M. Grätzel, S. Mhaisalkar, and T. C. Sum, Nat. Mater. **13**, 476 (2014).
[6]J. Zhang, Q. Zhang, X. Wang, L. C. Kwek, and Q. Xiong, Nat. Photon. **10**, 600 (2016).
[7]T. M. Brenner, D. A. Egger, L. Kronik, G. Hodes, and D. Cahen, Nat. Rev. Mater. **1**, 15007 (2016).
[8]D. Shi, V. Adinolfi, R. Comin, M. Yuan, E. Alarousu, A. Buin, Y. Chen, S. Hoogland, A. Rothenberger, K. Katsiev, Y. Losovyj, X. Zhang, P. A. Dowben, O. F. Mohammed, E. H. Sargent, and O. M. Bakr, Science **347**, 519 (2015).
[9]J. S. Manser, J. A. Christians, and P. V. Kamat, Chem. Rev. **116**, 12956 (2016).
[10]M. Saliba, T. Matsui, J.-Y. Seo, K. Domanski, J.-P. Correa-Baena, M. K. Nazeeruddin, S. M. Zakeeruddin, W. Tress, A. Abate, A. Hagfeldt, and M. Gratzel, Energy Environ. Sci. **9**, 1989 (2016).
[11]N. J. Jeon, J. H. Noh, Y. C. Kim, W. S. Yang, S. Ryu, and S. I. Seok, Nat. Mater. **13**, 897 (2014).
[12]A. Mei, X. Li, L. Liu, Z. Ku, T. Liu, Y. Rong, M. Xu, M. Hu, J. Chen, Y. Yang, M. Grätzel, and H. Han, Science **345**, 295 (2014).
[13]N. Ahn, D.-Y. Son, I.-H. Jang, S. M. Kang, M. Choi, and N.-G. Park, J. Am. Chem. Soc. **137**, 8696 (2015).
[14]A. Priyadarshi, L. J. Haur, P. Murray, D. Fu, S. Kulkarni, G. Xing, T. C. Sum, N. Mathews, and S. G. Mhaisalkar, Energy Environ. Sci. **9**, 3687 (2016).
[15]D. P. McMeekin, G. Sadoughi, W. Rehman, G. E. Eperon, M. Saliba, M. T. Hörantner, A. Haghighirad, N. Sakai, L. Korte, B. Rech, M. B. Johnston, L. M. Herz, and H. J. Snaith, Science **351**, 151 (2016).
[16]G. R. Yettapu, D. Talukdar, S. Sarkar, A. Swarnkar, A. Nag, P. Ghosh, and P. Mandal, Nano Lett. **16**, 4838 (2016).
[17]L. M. Herz, Annu. Rev. Phys. Chem. **67**, 65 (2016).
[18]M. B. Johnston and L. M. Herz, Acc. Chem. Res. **49**, 146 (2016).
[19]C. Wehrenfennig, G. E. Eperon, M. B. Johnston, H. J. Snaith, and L. M. Herz, Adv. Mater. **26**, 1584 (2014).
[20]G. Xing, B. Wu, X. Wu, M. Li, B. Du, Q. Wei, J. Guo, E. K. L. Yeow, T. C. Sum, and W. Huang, Nat. Commun. **8**, 14558 (2017).
[21]J. Li, G. Niu, W. Li, K. Cao, M. Wang, and L. Wang, Nanoscale **8**, 14163 (2016).
[22]T.-B. Song, Q. Chen, H. Zhou, C. Jiang, H.-H. Wang, Y. Yang, Y. Liu, J. You, and Y. Yang, J. Mater. Chem. A **3**, 9032 (2015).
[23]W. Junke, D. G. Francesco, B. Jim, G. Harrie, K. Ilias, G. Pim, J. R. A. J., A. Ronn, and G. Yulia, Solar RRL **1**, 1700091 (2017).